Supplemental Material
Table of Contents

Data	Page #
Supplemental Methods 1- Eligibility Criteria 2- Study Design 3- Laboratory measurements 4- DXA, trabecular bone score and HR-pQCT Measurements 5- Bone Biopsy and Histomorphometry and Analysis of Bone Tissue Properties 6- Sample Size Calculation	 Page 2 Pages 2,3 Page 3 Pages 4,5 Pages 5,6 Pages 6,7
Supplemental Table 1. Relationships between post-treatment changes in levels of PTH, bone specific alkaline phosphatase and C-Telopeptide and post-treatment changes in bone imaging using mixed linear models adjusted for baseline bone imaging and biochemical measures	Page 8
Supplemental Table 2. Phosphate binders, vitamin D supplement and vitamin D receptor analog use at baseline and at study completion.	Page 9
Supplemental Table 3. Doses of phosphate binders and vitamin D receptor analogues at baseline and at study completion.	Page 10
Supplemental Table 4. Biochemical and bone imaging baseline, follow-up and change data throughout the trial for the participants who underwent a bone biopsy.	Pages 11,12
Supplemental Figure 1. Study outline for assessments of measures collected over 36-weeks of study participation.	Page 13
Supplemental Figure 2. Median levels of serum intact parathyroid hormone (PTH) obtained by the hemodialysis unit for clinical management	Page 14
Supplemental Figure 3. Quadruple label method to assess dynamic indices of histomorphometry. Tetracycline double label was used at baseline prior to initiation of etelcalcetide (white arrow, green fluorescence) and Declomycin double label was used 36-weeks after treatment (red arrow, blue-green fluorescence). Dynamic indices of histomorphometry were assess between the individual labels.	Page 15
Supplemental Figure 4. Dynamic measures of histomorphometry in cortical bone from quadruple-label bone biopsy before and after 36-weeks of etelcalcetide treatment	Page 16
Supplemental Figure 5. Bone material strength measured by Nano-Indentation in trabecular bone before and after 36-weeks of etelcalcetide treatment	Page 17
Supplemental Figure 6. Bone crystal and collagen properties measured by Raman Spectroscopy before and after 36-weeks of etelcalcetide treatment	Page 18
References	Page 19

1- Eligibility Criteria

Men and women were eligible for enrollment if they had end-stage kidney disease (ESKD), ≥18 years of age, stable on hemodialysis ≥ 3 months, had PTH levels > 9-times the upper limit of normal (ULN) of the local parathyroid hormone (PTH) reference range (80 pg/mL; > 721 pg/mL) measured on two separate days within 2 weeks prior to enrollment, had corrected serum calcium levels within the local reference range measured within 2 weeks of enrollment, were on stable doses of vitamin D sterols within 4 weeks of enrollment, were on stable doses of calcium supplements and phosphate binders within 2 weeks of enrollment, and were clinically indicated to receive a calcimimetic for treatment of severe hyperparathyroidism. Study participants were eligible to enroll in the bone biopsy sub-study if they had suspected high turnover bone disease based on total alkaline phosphatase ≥ the upper tertile of local assay reference range (46-116 U/L; ≥ 92 U/L). Patients were not eligible for enrollment if they had received cinacalcet or parathyroidectomy in the 6 months prior to screening procedures, were scheduled to receive parathyroidectomy or kidney transplantation during the course of the study, had bilateral lower extremity amputations that would preclude performance of HR-pQCT imaging, had metabolic bone disease unrelated to CKD, malignancy within 5 years prior to screening, or if the patient was pregnant, nursing or refused to take highly effective contraception over the course of the study (for those with reproductive potential).

2- Study Design

After enrollment, all study participants had pre-treatment collection of blood and skeletal imaging. This was followed by a 12-week etelcalcetide dose titration phase to target a PTH level at approximately the lower half of the recommended reference range (2-5 times the ULN for the local PTH assay; 160 to 400 pg/mL; Supplemental Figure 2). At the end of the titration phase, participants entered a 24-week treatment phase; goal PTH levels were to be maintained within the target range. Patients had intra-treatment bloods obtained at 24-weeks, and at 36-weeks and post-treatment collection of blood and skeletal imaging. All blood was frozen and stored at -80º C for batch assay at end of study. During the titration and treatment phases, doses of etelcalcetide, calcium and vitamin D sterols were permitted to be adjusted according to treating physician decision-making to

maintain corrected calcium levels within the normal reference range. Biochemical data (i.e., PTH, corrected calcium) used to dose titrate and monitor administration of etelcalcetide, calcium and vitamin D sterols, was from clinical bloods obtained according to standard hemodialysis practice patterns.

Patients who agreed to participate in the quadruple-label bone biopsy sub-study underwent tetracycline double labeling at baseline (before etelcalcetide administration). Tetracycline 250 mg four-times daily was given on the following schedule: 3 days on, 12 days off, 3 days on. The etelcalcetide titration phase began after the first labeling procedure was completed. At 36-weeks, at study endpoint, patients were given the second label of demeclocycline 150 mg 4-times daily on the following schedule: 3 days on, 12 days off, 3 days on. Bone biopsy was obtained after the second labeling procedure was completed. During the second labeling period, patients were maintained on etelcalcetide to maintain PTH suppression.

3- Laboratory Measurements

All routine laboratories used for hemodialysis management and clinical decision making (i.e., for etelcalcetide dosing and monitoring) were measured by Spectra Labs till December 2019 and then Ascend Labs going forward for the remained of the study. These assays included intact PTH and serum calcium. All research blood samples were obtained prior to hemodialysis after the long inter-dialysis period, stored at -80ºC and batch assayed at the end of study. Whole PTH (1-84) and bone turnover markers and hormones were measured in the Bone Biomarker Laboratory in the CUIMC CTSA. Whole PTH 1-84 was measured in plasma by Scantibodies immunoradiometric assay (Scantibodies Laboratory, Santee, CA, USA), bone specific alkaline phosphatase was measured in serum by ELISA (Quidel, San Diego, CA, USA). C-Telopeptide was measured in serum by ELISA (IDS, Tyne & Wear, UK). Intact and c-terminal FGF-23 were measured in serum by ELISA (Quidel, San Diego, CA, USA). Sclerostin was measured in serum by ELISA (Quidel, San Diego, CA, USA). Inter- and intra-assay precisions are reported as: whole PTH 2.93-7.76% and 2.3-6.05%; bone specific alkaline phosphatase 5-8% and 4-6%; Serum cross-linked C-telopeptide of type I collagen 7.7% and 2.17%, FGF-23 c-terminal 3.5-9.1% and 2.0-4.1%, FGF-23 c-terminal 2.4-4.7% and 1.4-2.4%, and Sclerostin 4.3-4.8% and 3.7-4.2%, respectively. Pre-menopausal reference ranges are reported in Table 2 from manufacturer assay insert or the literature[1,2] for comparative purposes.

4- DXA, Trabecular Bone Score and HR-pQCT Measurements

Areal bone mineral density by DXA was measured at the total lumbar spine (L1 through L4), total hip, femoral neck, and non-dominant 1/3 and ultradistal radius using a Hologic Horizon densitometer (Hologic, Inc., Waltham, MA) in the array (fan beam) mode. In our laboratory, short-term, *in vivo* precision is 0.68% for the spine, 1.36% for the femoral neck, and 0.70% for the radius. Z-Scores compared participants to data from populations of the same age and sex provided by the manufacturer (spine and forearm) and by the National Health and Nutrition Examination Survey III (total hip and femoral neck). Spine trabecular bone score parameters were extracted from the DXA image using trabecular bone score iNsight software (version 3.0.3; Medimaps Group; Geneva, Switzerland).

Volumetric bone mineral density and microarchitecture were measured at the distal radius and tibia using the second-generation HR-pQCT scanner (XCT2; Scanco Medical AG, Brüttisellen, Switzerland) using a microfocus x-ray source with an isotropic voxel size of 61 µm (68kVp voltage, 900 µA current, 43 sec integration time). The non-dominant forearm and leg were scanned unless there was previous fracture or an arteriovenous fistula or graft at the desired site in which case the opposite limb was scanned. The region of interest was defined on a 2D scout view by placing the reference line at the proximal and distal endplate for radius and tibia respectively. A 10.2 mm long scan region was acquired along the length of the bone at a relative offset from the reference line; 4% and 7.3% of limb length for radius and tibia respectively. A more proximal diaphyseal scan at 30% relative offset was also acquired at the tibia, comprised mostly of cortical bone. All scan acquisition and analysis were performed in our laboratory by a single dedicated research densitometrist. Attenuation data were converted to equivalent hydroxyapatite (HA) densities. A phantom was scanned daily for quality control. Manufacturer's standard method was used to filter and binarize the images. An automated segmentation algorithm with dual threshold and a series of morphological operations was used to separate the cortical and trabecular regions.[3] HR-pQCT outcomes relating to geometry, density and microstructure were computed namely – total, trabecular and cortical (Ct) density, trabecular number, thickness, separation and heterogeneity, cortical thickness, porosity and pore size.[4] For longitudinal analysis, manufacturer's cross-sectional area matching was used to analyze the same region in each scan.[5] *In vivo* short-term precision of HR-pQCT measurements is between

0-5% for all measures except cortical porosity (unpublished data). All HR-pQCT scans were assessed for image quality and motion artifact prior to analysis and were graded on a scale of 0 (no imaging abnormalities) to 5 (severe abnormalities)[6,7] and scans with motion score >3 were excluded from analyses.

Estimated bone strength (stiffness and failure load) was estimated from the HR-pQCT images using micro-finite element analysis (μFEA) based on a voxel conversion approach. Axial compression was simulated up to 1% strain using a homogenous Young's modulus of 10 GPa and Poisson's ratio of 0.3. The μFEA solver used was provided by the manufacturer (Scanco Medical FE software v1.13, Scanco Medical AG, Brüttisellen, Switzerland).

5- Bone Biopsy and Histomorphometry and Analysis of Bone Tissue Properties

This study utilized a quadruple-label transiliac crest biopsy method to assess treatment effects while maximizing patient safety, recruitment and adherence to bone biopsy procedures. Because two different tetracyclines are used that fluoresce in different colors, a single biopsy can be used to assess dynamic indices of bone before and after intervention (Supplemental Figure 3).[8,9] Biopsies from five patients were collected into 70% ethanol and shipped to the Indiana University School of Medicine (IUSM) for processing and analyses. Specimens were serially dehydrated and embedded in methyl methacrylate using standard protocols. Four-micron thick sections were cut with a rotary microtome and left unstained for dynamic histomorphometry or stained with McNeal tetrachrome or tartrate resistant acid phosphatase (TRAP) for static measures. A region of interest including all trabecular bone and excluding cortical bone was analyzed separately for each label. Standard analysis techniques were used to measure single, double and no labelled surfaces and distances between the two labels of each fluorescence. Standard calculations of mineral apposition rate (um/day), mineralizing surface/bone surface (%) and bone formation rate/bone surface (um3/um2/year) were made. Both cortices were analyzed for intracortical measures included mineral apposition rate, and bone formation rate/bone surface (%/year). Static parameter assessment included measures of osteoid surface and thickness, and osteoclast surface. All histological measures were done in accordance with ASBMR recommendations.

Biopsies underwent colocalized Raman spectroscopy and nanoindentation using a custom hybrid system to assess composition and nano-mechanical properties between the two different labels within trabecular bone. Embedded biopsies blocks were polished using a 3 μm diamond suspension. A coordinate system was placed on the image guiding point selection for colocalized Raman spectroscopy and nanoindentation. This included 6 locations between each set of fluorochrome labeling. Raman spectra were acquired with a 785 nm laser using a 9-second exposure, 50% laser power, and a grating resolution of 1200 I/mm (633/780), where ~8 accumulations were collected and averaged at each point (InVia Raman Spectrometer, Renishaw, Wotton-under-Edge, United Kingdom). Spectra were baseline corrected using an 11th order polynomial, cosmic rays were removed, and smoothed using a modified Savitzky-Golay function. Compositional parameters were calculated from the spectrographs including type B carbonate substitution (ν1-CO32-/ν1-PO43- band areas and intensities), mineral crystallinity (inverse of the full width at half maximum of ν1-PO43-), and mineral-to-matrix ratios for Amide I band (ν1-PO43-/Amide I band areas and intensity), Amide III band (ν1-PO43-/Amide III band areas and intensity), and CH2 wagging (ν1-PO43-/ CH2 wagging areas and intensity). The output parameters were averaged over the points for each label yielding one value per parameter per timepoint per biopsy.

Following Raman spectroscopy, samples underwent nanoindentation using a Hysitron TI 980 TriboIndenter (Bruker, Billerica, MA) equipped with a diamond Berkovich probe. Indents were performed at the same points as Raman spectroscopy. The loading profile consisted of a 30 second loading period followed by a 60 second hold at 1,000 μN, and a 30 second unloading period with a displacement rate of 200 μN/second. Load-displacement curves were analyzed for reduced modulus and hardness as previously described. The data were averaged to produce a single value for of the two labels on each biopsy.

6- Sample Size Calculation

The *a priori* primary outcome was the percent change in DXA areal bone mineral density at the femoral neck. Secondary outcomes included changes in: (1) areal bone mineral density of the spine by DXA and total hip by DXA; (2) trabecular bone score and (3) HR-pQCT outcomes (i.e., radius and tibia cortical and trabecular

volumetric density, microarchitecture, geometry and stiffness and failure load). Bone histomorphometric measures were assessed for bone tissue safety, including bone formation and mineralization rates and hardness. Based on previous studies,[10,11] our original estimates required 35 study participants to obtain 80% power at a 5% alpha to detect a 0.68-SD effect size consistent with a 0.5% change in areal bone mineral density at the femoral neck, or a 3.5% change in radius failure load or stiffness by HR-pQCT. Due to early study termination (Figure 1), thirteen patients completed imaging procedures and sample size recalculations indicated the minimum detectable difference at 80% power and 0.05 alpha increased to a 1.14-SD effect size with the reduced sample size. This effect size corresponds to a 1.8% increase in areal DXA femoral neck bone mineral density , a 4.79% increase in HR-pQCT radius stiffness and a 4.1% radius failure load. Five patients completed the bone biopsy protocol and histomophometric analyses are presented to demonstrate effects on bone turnover and tissue quality.

Supplemental Table 1. Relationships between post-treatment changes in levels of PTH, bone specific alkaline phosphatase and C-Telopeptide and post-treatment changes in bone imaging using mixed linear models adjusted for baseline bone imaging and biochemical measures

	Baseline PTH	Δ PTH	Baseline BSAP	Δ BSAP	Baseline CTX	Δ CTX
DXA						
Lumbar Spine	-0.00136	***0.05635****	0.03113	***0.1243****	-0.00896	***0.1147****
Femoral Neck	0.003	-0.051	0.0199	-0.112	0.356	-0.0354
Total Hip	-0.00075	0.03548	0.02759	0.05882	-0.04799	0.07881
One-Third Radius	-0.00079	***-0.06524****	-0.01888	***-0.1148****	0.217	-0.06143
Ultra-Distal Radius	-0.00026	-0.01772	-0.01441	-0.03858	-0.1056	0.00309
TBS	-0.0059	-0.0516	-0.01461	-0.1339	0.1865	-0.04825
HR-pQCT Radius						
Stiffness	-0.0128	0.017	0.0239	0.0822	0.9178	0.0981
Failure Load	-0.01149	0.0536	0.03362	0.08128	0.6646	0.13
Total Density	0.002322	***0.06248****	0.0312	-0.09535	-0.00413	0.05226
Cortical Area	0.000913	-0.00973	-509	***-0.03453****	0.04643	***-0.04819****
Cortical Density	-0.0155	-0.3469	-0.1197	-0.5355	0.1362	-0.01888
Cortical Perimeter	0.00036	-0.00088	0.000965	-0.00602	0.01317	-0.0041
Cortical Thickness	0.00049	***-0.03392****	***-0.01996****	***-0.06376****	0.02956	***-0.06164*****
Cortical Porosity	0.000013	0.000101	-0.1043	-0.1133	0.000266	0.000187
Diameter	-0.01424	-0.05742	-0.0054	-0.07143	0.000532	0.000078
Trabecular Area	-0.00059	-0.00415	-0.00362	0.007515	-0.00147	0.001769
Trabecular Density	-0.00108	***0.1702*****	***0.07322****	0.08088	-0.3294	***0.2315****
Trabecular Thickness	0.003205	0.01094	0.006234	-0.02118	-0.2268	0.01174
Trabecular Number	-7.26E-06	***0.05938****	0.02484	-0.04722	-0.186	0.03659
Trabecular Spacing	-0.00131	***-0.06558****	-0.0248	0.09316	0.1345	-0.04169
Trabecular Heterogeneity	-0.00882	-0.05904	-0.01314	***0.2850****	-0.01775	-0.00446
HR-pQCT Tibia						
Stiffness	0.000876	***0.1372*****	***0.0697****	0.1158	-0.1855	***0.1848****
Failure Load	0.001	***0.1345*****	***0.06747****	0.1146	-0.1179	***0.1775****
Total Density	0.000634	***0.1170*****	0.04422	***0.1325****	-0.248	***0.1461****
Cortical Area	0.006868	0.04878	0.01866	-0.00509	-0.03728	0.02507
Cortical Density	0.003931	***-0.1911****	-0.1088	***-0.3698****	0.07282	***-0.03248****
Cortical Perimeter	0.00045	0.00731	0.005712	0.006264	0.01508	***0.01773****
Cortical Thickness	0.003438	0.01582	0.001462	-0.01818	-0.04262	0.004816
Cortical Porosity	-8.60E-07	***0.000051*****	0.08931	***0.2981****	-0.00009	***0.00009*****
Diameter	-0.00332	-0.01472	-0.01305	0.08229	-0.00015	0.0001
Trabecular Area	-0.00028	***-0.00759****	-0.00362	-0.00803	0.01681	-0.00786
Trabecular Density	-0.00052	***0.2348*****	0.09499	***0.3491****	-0.3419	***0.3328*****
Trabecular Thickness	0.000228	***0.03737****	***0.02068****	***0.06373****	-0.03348	***0.05042****
Trabecular Number	0.001406	***0.03869****	0.01117	***0.1187*****	-0.06796	***0.06986****
Trabecular Spacing	0.000932	***-0.05214*****	0.09499	***0.3491****	-0.3419	***0.3328*****
Trabecular Heterogeneity	0.01166	***-0.09942****	0.02926	***-0.3123****	***0.7815****	***-0.1943****

p-value<0.05

****p-value<0.01***

*****p-value<0.001***

Supplemental Table 2. Phosphate binders, vitamin D supplement and vitamin D receptor analog use at baseline and at study completion.

Medications	Participants at Baseline (n=13)	Participants at 36-week Follow up (n=13)	p-value
Calcium acetate	1 (8%)	4 (13%)	0.2
Calcium carbonate	1 (8%)	7 (54%)	0.03
Sevelamer	7 (54%)	6 (46%)	1
Vitamin D2/D3 Supplement	5 (39%)	4 (31%)	1
Vitamin D receptor analog	11 (85%)	14 (100%)	0.5

Supplemental Table 3. Doses of phosphate binders, vitamin D receptor analogs, and calcium supplements at baseline and at study completion

Medication					
Phosphate Binders	**N**	**Mean Dose/Meal at Baseline (mg)**	**N**	**Mean Dose/Meal at 36-weeks Follow-Up (mg)**	**p-value**
Calcium acetate*	1	667	4	1834 +/- 839	
Sevelamer	7	1943 +/- 781	6	2000 +/- 980	0.9
Vitamin D Receptor Analogs	**N**	**Mean Weekly Dose at Baseline (mcg)**	**N**	**Mean Weekly Dose at 36-weeks Follow-Up (mcg)**	**p-value**
Calcitriol (oral)	6	2.0 +/- 1.5	9	2.2 +/- 1.3	0.8
Doxercalciferol (intravenous)	4	11.8 +/- 6	5	10.8 +/- 7.5	0.8
Calcium Supplementation	**N**	**Mean Weekly Dose at Baseline (mg)**	**N**	**Mean Weekly Dose at 36-weeks Follow-Up (mg)**	
Calcium supplement	1	31500	7	111386 +/- 10885	

* Calcium acetate has 325 mg of elemental calcium per 667 mg dose.

Supplemental Table 4. Biochemical and bone imaging baseline, follow-up and change data throughout the trial for the participants who underwent a bone biopsy				
Biochemicals	**Baseline Visit**	**36-Weeks Visit**	**Change (%)**	**p-value**
Whole PTH 1-84 (pg/mL)**	617 (482, 715)	282 (130, 181)	-55 +/- 21	0.1
Calcium (mg/dL)	9.4 (9, 9.8)	9.2 (8.4, 9.4)	-2 +/- 4	0.2
Phosphate (mg/dL)	6.0 (5.0, 6.9)	6.1 (5.9, 6.7)	13 +/- 20	0.9
BSAP (U/L)**	62 (42, 62)	40 (22, 42)	-39 +/- 5	0.2
C-Telopeptide (ng/mL)****	6.2 (3.8, 6.9)	3.3 (0.6, 5.9)	-54 +/- 13	0.2
FGF23 C-terminal (RU/mL) ***	6290 (2419, 9404)	6805 (1234, 11166)	-2 +/- 23	0.9
FGF23 Intact (pg/mL) ***	7473 (1785, 11053)	8114 (1018, 12068)	-12 +/- 23	0.9
Sclerostin (ng/mL)****	1.7 (1.1, 2.5)	2.3 (1.4, 3.3)	43 +/- 17	0.4
Areal Bone Mineral Density (mg HA/cm^2)				
Lumbar Spine	1.00 +/- 0.16	1.02 +/- 0.16	2 +/- 2	0.9
Femoral Neck	0.73 +/- 0.12	0.77 +/- 0.12	7 +/- 3	0.5
Total Hip	0.86 +/- 0.13	0.89 +/- 0.10	3 +/- 2	0.8
⅓ Radius	0.63 +/- 0.11	0.63 +/- 0.13	-0.7 +/- 2	1.0
Ultra-Distal Radius	0.37 +/- 0.09	0.37 +/- 0.09	0.1 +/- 3	1.0
Spine Trabecular Bone Score				
Trabecular Bone Score	1.1 +/-	1.2 +/-	11 +/- 2	0.2
HR-pQCT at the radius				
Stiffness	40244 +/- 10380	44557 +/- 14240	10 +/- 10	0.6
Failure Load	2176 +/- 530	2404 +/- 779	10 +/- 9	0.6
Cortical area	43 +/- 11	42 +/- 10	-3 +/- 2	0.9
Cortical thickness	0.73 +/- 0.25	0.71 +/- 0.24	-2 +/- 2	0.9
Cortical Pore Diameter	0.16 +/- 0.02	0.17 +/- 0.02	5 +/- 5	0.6

Trabecular endocortical area	138 +/- 44	139 +/- 43	0.5 +/- 0.4	1.0
Trabecular number	1.5 +/- 0.4	1.4 +/- 0.3	-2 +/- 2	0.8
HR-pQCT at the tibia				
Stiffness	142435 +/- 25213	143479 +/- 17577	2 +/- 5	0.9
Failure Load	7810 +/- 1381	7863 +/- 957	2 +/- 5	0.9
Cortical area	243 +/- 47	246 +/- 46	0.1 +/- 2	0.9
Cortical thickness	4.8 +/- 1.1	4.9 +/- 1.1	0.1 +/- 2	1.0
Cortical Pore Diameter	0.20 +/- 0.03	0.20 +/- 0.05	2 +/- 2	0.8
Trabecular endocortical area	330 +/- 60	327 +/- 64	0.1 +/- 0.4	0.9
Trabecular number	1.1 +/- 0.2	1.1 +/- 0.2	0.04 +/- 1	0.7

N =5 for all cells except N =4 for HRpQCT at the tibia at the 36-weeks visit
Cell contents are median (IQR), mean (SD), or percent change (+/- SEM).

*healthy population reference range *5 - 39 pg/mL*
**pre-menopausal reference range BSAP11.6 - 29.6 U/L, C-Telopeptide 0.112- 0.738 ng/mL, Sclerostin Range 0.026 – 0.273 ng/mL
***no reference ranges reported

Supplemental Figure 1. Study outline for assessments of measures collected over 36-weeks of study participation.

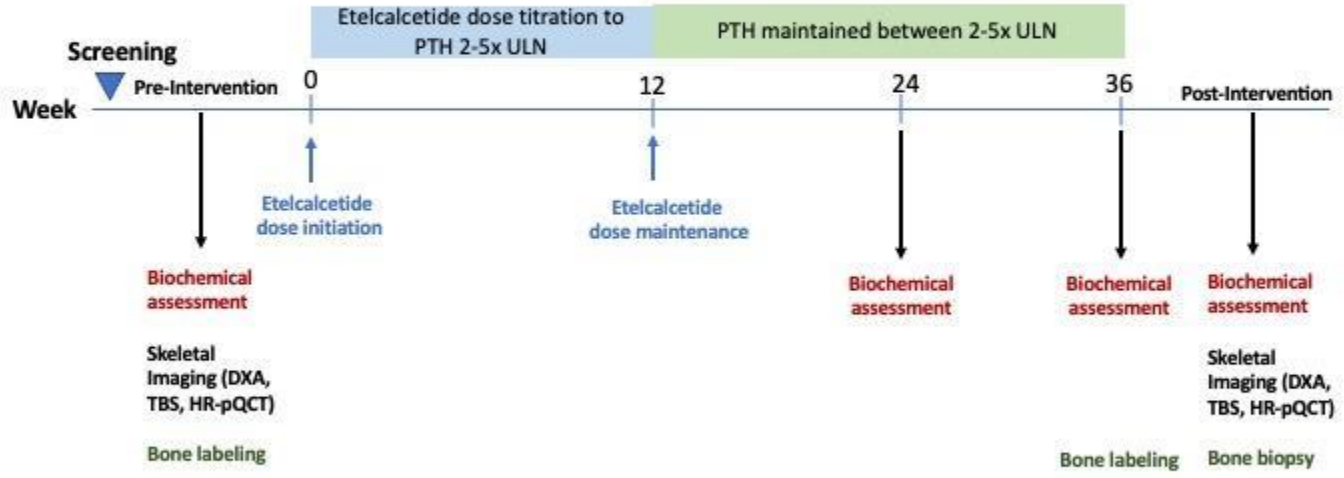

Supplemental Figure 2. Median levels of serum intact parathyroid hormone (PTH) obtained by the hemodialysis unit for clinical management at study initiation and 4-, 8-, 12-, 24- and 36-weeks of etelcalcetide administration. Grey box for PTH corresponds to the study target range (160 – 400 pg/mL).

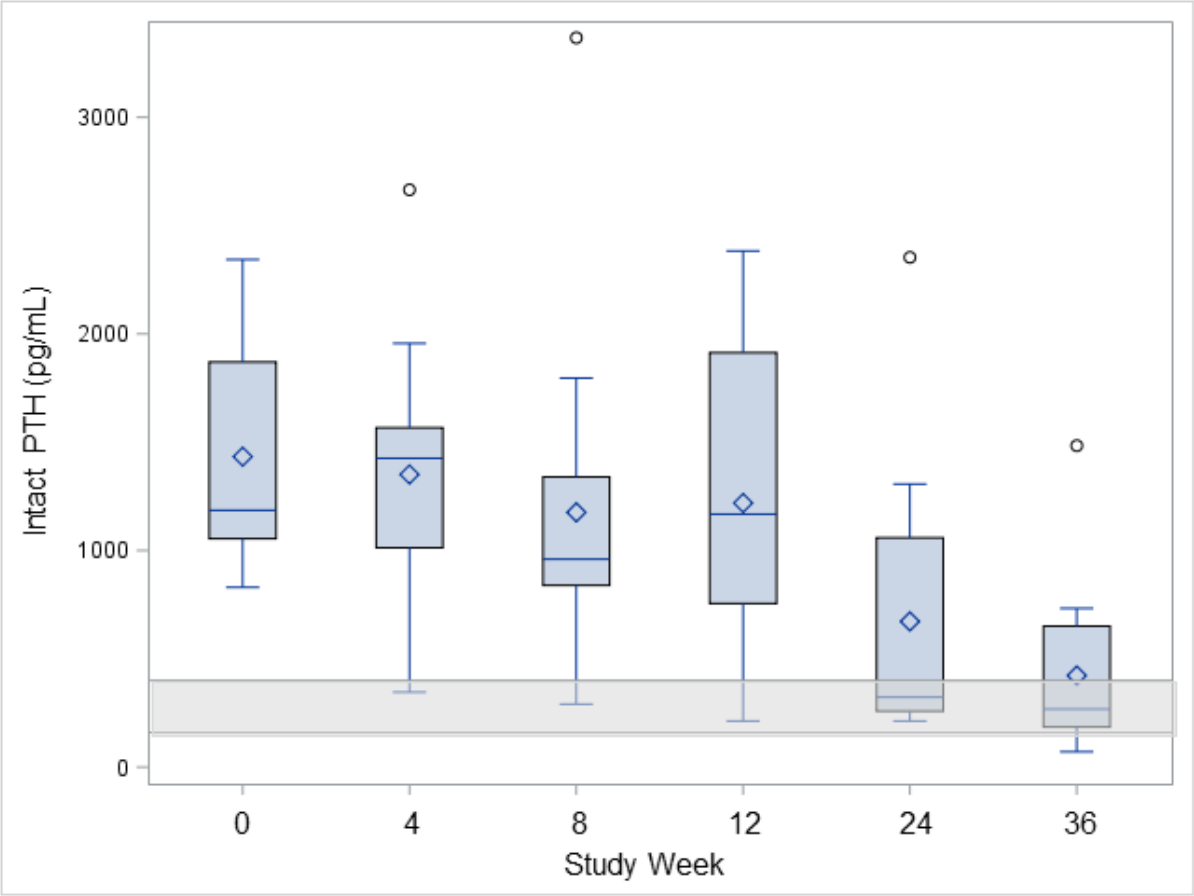

Supplemental Figure 3. Quadruple label method to assess dynamic indices of histomorphometry. Tetracycline double label was used at baseline prior to initiation of etelcalcetide (white arrow, green fluorescence) and Declomycin double label was used 36-weeks after treatment (red arrow, blue-green fluorescence). Dynamic indices of histomorphometry were assess between the individual labels.

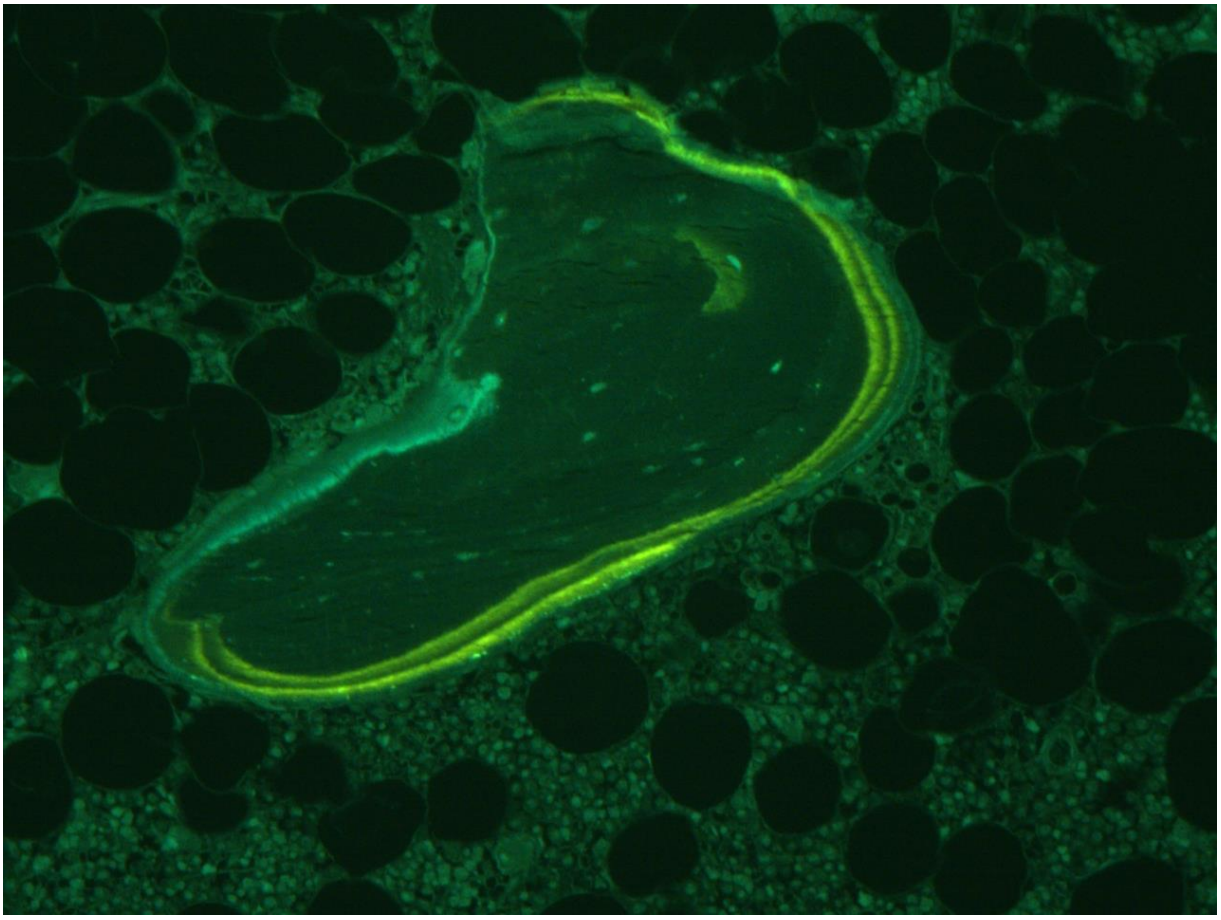

Supplemental Figure 4. Dynamic measures of histomorphometry in cortical bone from quadruple-label bone biopsy before and after 36-weeks of etelcalcetide treatment.

(a) Cortical Bone Formation Rate / Bone Surface (BFR/BS)

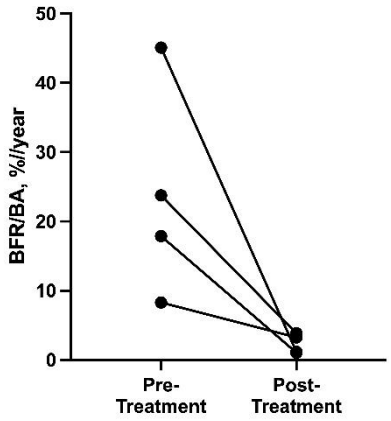

(b) Cortical Mineralizing Surface / Bone Surface Ratio

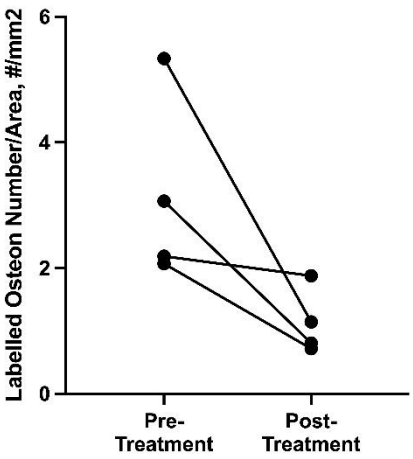

(c) Cortical Mineral Apposition Rate (MAR)

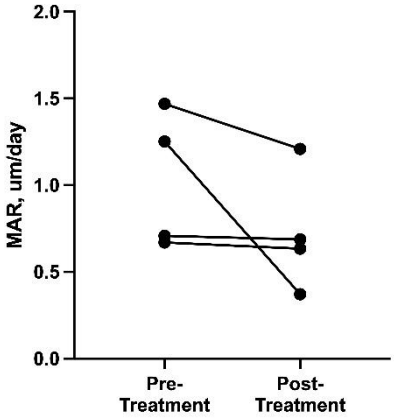

Supplemental Figure 5. Bone material strength measured by Nano-Indentation in trabecular bone before and after 36-weeks of etelcalcetide treatment

(a) Modulus

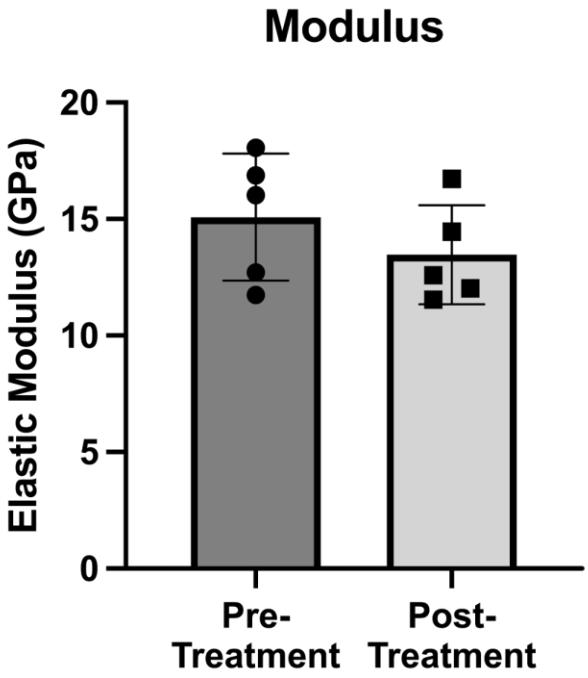

(b) Hardness

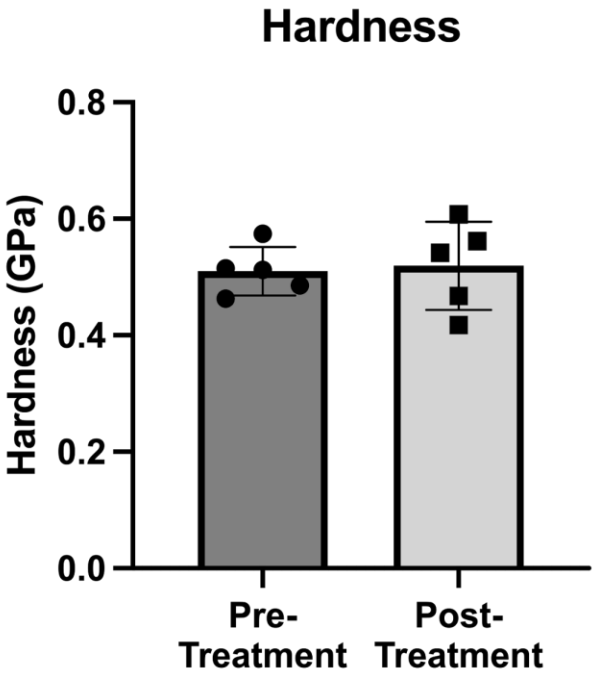

Supplemental Figure 6. Bone crystal and collagen properties measured by Raman Spectroscopy before and after 36-weeks of etelcalcetide treatment

(a) Carbonate Substitution Intensity

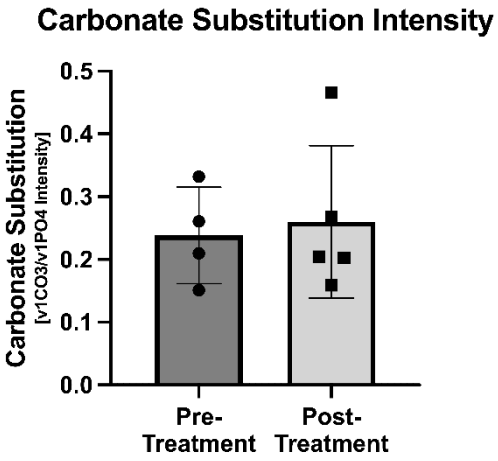

(b) Mineral Crystallinity / Maturity

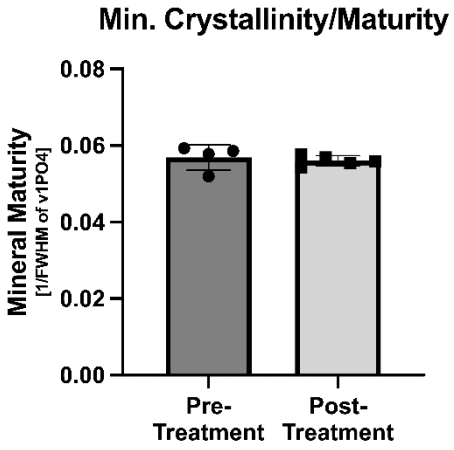

(c) Amide I Mineral-to-Matrix Ratio

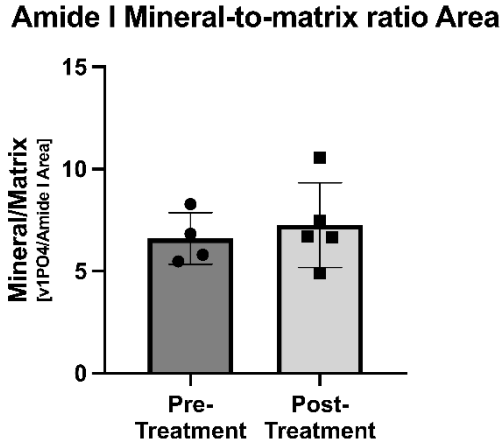

(d) Collagen Quality Index

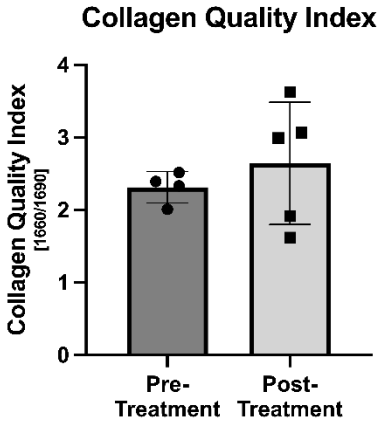

References

1. Michelsen J, Wallaschofski H, Friedrich N, Spielhagen C, Rettig R, Ittermann T, et al. Reference intervals for serum concentrations of three bone turnover markers for men and women. *Bone.* 2013;57(2):399-404.
2. Ardawi MS, Al-Kadi HA, Rouzi AA, Qari MH. Determinants of serum sclerostin in healthy pre- and postmenopausal women. *J Bone Miner Res.* 2011;26(12):2812-2822.
3. Buie HR, Campbell GM, Klinck RJ, MacNeil JA, Boyd SK. Automatic segmentation of cortical and trabecular compartments based on a dual threshold technique for in vivo micro-CT bone analysis. *Bone.* 2007;41(4):505-515.
4. Burghardt AJ, Buie HR, Laib A, Majumdar S, Boyd SK. Reproducibility of direct quantitative measures of cortical bone microarchitecture of the distal radius and tibia by HR-pQCT. *Bone.* 2010;47(3):519-528.
5. MacNeil JA, Boyd SK. Improved reproducibility of high-resolution peripheral quantitative computed tomography for measurement of bone quality. *Med Eng Phys.* 2008;30(6):792-799.
6. Pialat JB, Burghardt AJ, Sode M, Link TM, Majumdar S. Visual grading of motion induced image degradation in high resolution peripheral computed tomography: impact of image quality on measures of bone density and micro-architecture. *Bone.* 2012;50(1):111-118.
7. Sode M, Burghardt AJ, Pialat JB, Link TM, Majumdar S. Quantitative characterization of subject motion in HR-pQCT images of the distal radius and tibia. *Bone.* 2011;48(6):1291-1297.
8. Lindsay R, Cosman F, Zhou H, Bostrom MP, Shen VW, Cruz JD, et al. A novel tetracycline labeling schedule for longitudinal evaluation of the short-term effects of anabolic therapy with a single iliac crest bone biopsy: early actions of teriparatide. *J Bone Miner Res.* 2006;21(3):366-373.
9. Rubin M, Dempster D, Sliney J, Zhou H, Nickolas T, Stein E, et al. PTH(1-84) administration reverses abnormal bone remodeling dynamics and structure in hypoparathyroidism. *J Bone Miner Res.* 2011.
10. Lien YH, Silva AL, Whittman D. Effects of cinacalcet on bone mineral density in patients with secondary hyperparathyroidism. *Nephrol Dial Transplant.* 2005;20(6):1232-1237.
11. Iyer S NL, Nishiyama K, Dworakowski E, Cremers S, Zhang A, McMahon DJ, Boutroy S, Liu XS, Ratner L, Cohen D, Guo XE, Shane E, Nickolas TL. Kidney transplantation with early corticosteroid withdrawal: paradoxical effects at the central and peripheral skeleton. *J Am Soc Nephrol: in press.* 2014.